



Original article

Ailanthus altissima leaf extract mediated green production of zinc oxide (ZnO) nanoparticles for antibacterial and antioxidant activity



Shahid Shabbir Awan^a, Rizwan Taj Khan^a, Ansar Mehmood^{c,*}, Muhammad Hafeez^b, Syed Rizwan Abass^d, Munazza Nazir^a, Muhammad Raffi^e

^a Department of Botany, University of Azad Jammu and Kashmir, Muzaffarabad, Azad Kashmir, Pakistan

^b Department of Chemistry, University of Azad Jammu and Kashmir, Muzaffarabad, Azad Kashmir, Pakistan

^c Department of Botany, University of Poonch Rawalakot, 12350 Azad Jammu and Kashmir, Pakistan

^d Department of Biotechnology, Karakoram International University Gilgit, Pakistan

^e Department of Materials Engineering, National Institute of Lasers and Optronics (NILOP), Lehtrar Road, Nilore, Islamabad 45650, Pakistan

ARTICLE INFO

Article history:

Received 10 March 2022

Revised 14 September 2022

Accepted 25 October 2022

Available online 1 November 2022

Keywords:

Ailanthus altissima

ZnO

Nanoparticles

Antioxidant activity

Antibacterial activity

ABSTRACT

Background: Fabricating zinc oxide nanoparticles (ZnO-NPs) from plant extracts is a cost-effective, safe, and environmentally friendly alternative to established chemical procedures. This study was aimed at the environmentally friendly fabrication of ZnO-NPs from plant extract. An additional objective was to investigate the antibacterial and antioxidant activity of these biosynthesized ZnO-NPs.

Methods: ZnO-NPs were fabricated using the leaf extract of *Ailanthus altissima*, as an eco-friendly approach. The physicochemical properties of ZnO-NPs were explored using UV-visible spectroscopy, scanning electron microscopy, X-ray diffraction, and Fourier transform infrared spectrometry. The bio-fabricated ZnO-NPs were examined for bactericidal activity against pathogenic bacteria (gram-negative and gram-positive) using the agar well diffusion technique. The antioxidant efficiency of ZnO-NPs was assessed using a DPPH assay.

Results: A surface Plasmon peak was recorded at 327 nm, showing the existence of ZnO-NPs in the reaction solution of plant extract and zinc sulfate hexahydrate salt. These nanoparticles were predominantly spherical and capped by different functional groups of biomolecules. Furthermore, ZnO-NPs showed a dose-dependent antibacterial and antioxidant activity. At 20 mg/mL ZnO-NPs, the maximum bactericidal potential of ZnO-NPs was reported against *Staphylococcus aureus* (201.2 mm). ZnO-NPs have an IC₅₀ value of 78.23 µg/mL, indicating that they are an effective antioxidant.

Conclusion: This research presents an environmentally acceptable method for producing spherical ZnO-NPs with high antibacterial and antioxidant activities. These bio-fabricated ZnO-NPs could be a good option for applications in medicine and the healthcare industry.

© 2022 The Author(s). Published by Elsevier B.V. on behalf of King Saud University. This is an open access article under the CC BY-NC-ND license (<http://creativecommons.org/licenses/by-nc-nd/4.0/>).

1. Introduction

Nanoparticles (NPs) have a diversity of uses because of their unique properties in terms of size, shape, and surface area. The

most significant use of NPs is their application as catalytic agents (Valldeperas et al., 2016). In addition to catalysts, NPs of Nobel metals like gold, platinum, and zinc oxide are being widely used in medical and consumer products (Ishak et al., 2019). Moreover, NPs have the capability to mix with other organic molecules and absorb them, which is why they are considered chemical hazards (Surmenev et al., 2019). Besides many other applications of metal NPs, researchers are now looking at their antibacterial efficacy against multi-drug resistant bacteria. Because resistance is developing in pathogenic bacteria against existing drugs, combating these drug-resistant bacteria will be a leading challenge soon. It is found that inorganic materials, particularly metal NPs, can meet this challenge because of their antimicrobial properties and having the property of being more stable at harsh conditions and high

* Corresponding author.

E-mail addresses: shahid.shabbir@ajku.edu.pk (S. Shabbir Awan), rizwan.taj@ajku.edu.pk (R. Taj Khan), ansarmehmood@upr.edu.pk (A. Mehmood), muhhammad.hafeez@ajku.edu.pk (M. Hafeez), dr.syedrizwan@kiu.edu.pk (S. Rizwan Abass), munnaza.nazir@ajku.edu.pk (M. Nazir), raffi@nilop.edu.pk (M. Raffi).

Peer review under responsibility of King Saud University.



Production and hosting by Elsevier

<https://doi.org/10.1016/j.sjbs.2022.103487>

1319-562X/© 2022 The Author(s). Published by Elsevier B.V. on behalf of King Saud University.

This is an open access article under the CC BY-NC-ND license (<http://creativecommons.org/licenses/by-nc-nd/4.0/>).

temperatures as compared to organic materials (Zhang et al., 2007a,b). Various metal nanoparticles are now being tried in the hunt for more effective antibacterial agents, and zinc oxide nanoparticles (ZnO-NPs) are one of them. Brooks and Trifts (2008) describe how ZnO-NPs are used in food manufacture as a source of micronutrients and how they play a vital and effective function in human and animal growth, development, and health.

The antibacterial efficacy of NPs is determined by their size, shape, and manufacturing procedures. The NPs synthesized from plant extract can have better antibacterial efficacy because of different biomolecules that cap the NPs. Moreover, different plants have a different range of biomolecules, and NPs synthesized from different plants can have different antibacterial activities. Therefore, it is very important to synthesize nanoparticles from a new source (plant extract), which may increase the antibacterial efficiency of NPs. Other advantages of using plant extracts are that they are eco-friendly, cost-effective, and devoid of toxic chemicals during the synthesis procedure (Irvani, 2011). It has been observed that biosynthesized ZnO-NPs have greater repressing effects against pathogenic bacteria and fungi than chemically produced NPs (Gunalan et al., 2012).

In this study, we used the biomolecules extracted from leaves of *Ailanthus altissima* (Mill.) Swingle, as a source of reducing, capping, and stabilizing agent. *A. altissima* is a deciduous tree belonging to the family Simaroubaceae and native to Southeast Asia and India. Due to its ornamental value, this plant has been widely cultivated in Africa, Oceania, and Europe (Zhang et al., 2007a,b; Fogliatto et al., 2020) but it can be found in several countries across Europe and North America. It has been widely used to treat ophthalmic illnesses, ascariasis, spermatorrhea, bleeding, asthma, and epilepsy (Yang et al., 2014; Kim et al., 2016). The plant contains α -pinene, β -pinene, and α -terpinene as important chemical constituents and is used for the treatment of many diseases (Cao, 2004). Although the fruit extract of *A. altissima* has been used to synthesize ZnO-NPs (Awwad et al., 2020), but the synthesis of ZnO-NPs from leaf extract was the main focus of this investigation. It was hypothesized that aqueous leaf extract has the potential to synthesize the ZnO-NPs eco-friendly. Therefore, this study has 2-fold objectives, first is the green production and characterization of ZnO-NPs from the leaf aqueous extract of *A. altissima* and the second is the evaluation of ZnO-NPs for antibacterial and antioxidant activity.

2. Methods

2.1. Plant material and preparation of extract

The leaf extract of *Ailanthus altissima* was used for the synthesis of ZnO-NPs. The leaves were collected at the flowering stage when the plant was at its full bloom. The plant was found in Garhi Dupatta (34° 13' 32" N, 73° 36' 55" E), Muzaffarabad, Azad Kashmir, Pakistan. The choice of the leaves was made based on their availability and active metabolic components. The leaves were cleaned with distilled water, air dried, and ground to a fine powder with an electric grinder. A 10 g powder was mixed with 1 L deionized water and boiled at 80 °C for 10 min and then left at room temperature for cooling down. Whatman's filter paper (1 μ) was used to filter the extract, which was then saved for future research.

2.2. Synthesis of ZnO-NPs

The synthesis of ZnO-NPs was carried out by following the procedure adopted by Nilavukkarasi et al. (2020) with some modifications. The solution of zinc sulfate hexahydrate salt (Purum 98 ZnSO₄·6H₂O) was prepared by dissolving it in 200 mL of deionized water having a resistivity of 18.2 megohms in a measuring

flask by constant stirring using a magnetic stirrer. For ZnO-NPs fabrication, 50 mL of leaf filtrate from the plant was treated with a zinc salt solution with continuous heating and stirring for 20 mins. The pH of the reaction solution was controlled by adding the 0.1 M NaOH until the color of the mixture changed and suspended particles were formed. The reaction solution was left for 24 h and filtered to get the ZnO-NPs. It was then dried at 80 °C in an oven for 4 h to get the powdered ZnO-NPs.

2.3. Characteristics of synthesized ZnO-NPs

The initial step of the synthesized NPs is the recognition of their structure, properties, and reaction mechanism. For this, different characterization techniques have been used. The absorption spectrum in the UV-Visible range of the fabricated ZnO-NPs was recorded using a Shimadzu UV-1601 UV-visible spectrophotometer. The surface morphology and particle size were established using Tescan Maia 3 scanning electron microscopy (SEM). The sample was characterized using a Shimadzu X-ray diffractometer (XRD-6000) using Cu-K α radiation as a source of X-rays with a wavelength of $\lambda = 1.541 \text{ \AA}$ to determine the crystallinity of ZnO-NPs. The capping agents of ZnO-NPs were identified using Fourier transform infrared spectroscopy (FTIR) of IR Prestige-21, Shimadzu.

2.4. Antibacterial activity of ZnO-NPs

An agar well diffusion assay was used to test the bactericidal activity of manufactured ZnO-NPs. (Manjunath et al., 2014). All the reagents and equipment were autoclaved before use. The standard antibiotic Clindamycin phosphate was used as a positive control. This antibiotic works by stopping the growth of bacteria. Clindamycin phosphate is actively used for the treatment of dental infections because of its action against anaerobic bacteria. The bacterial isolates were brought from the Combined Military Hospital (CMH) Muzaffarabad in inactive form. They were activated in the lab and treated as test organisms to evaluate the antibacterial effects of ZnO-NPs. Four different strains were used for antimicrobial action, namely *Staphylococcus aureus*, *Klebsiella pneumoniae*, *Escherichia coli*, and *Streptococcus pyogenes*. Briefly, five wells (6 mm in diameter) were created by gel puncture on Mueller-Hinton agar plates. Each bacterial strain was mopped on the individual Petri plate uniformly with the help of sterilized cotton swabs. With the help of a micropipette, 5, 10, and 20 mg/mL of ZnO-NPs solution flowed onto each of 3 wells on all plates, while the other 2 wells were filled with antibiotic clindamycin and dimethyl sulfoxide (DMSO), which acted as a control. The different values of the zone of inhibition were evaluated using a measuring scale after incubation for 24 h at 37 °C. All the steps were repeated thrice, and the average zone of inhibition was obtained.

The antibacterial activity was further verified with minimum inhibitory concentration (MIC) using broth dilution. ZnO-NPs were serially diluted at concentrations of 0.3125, 0.625, 1.25, 2.50, 5.0, 10, and 20 mg/mL. Different ZnO-NPs concentrations, 10 mL samples of nutrient broth, and 100 μ L of active bacterial suspension inoculums (1.5×10^8 CFU/mL) were added to test tubes and then incubated at 37 °C for 24 h. The least amount of plant extract needed to stop bacterial growth is known as the MIC. The lack of growth was demonstrated by the absence of turbidity and inoculation on agar-containing Petri dishes.

2.5. Antioxidant activity of ZnO-NPs

The antioxidant efficiency of the ZnO-NPs was determined using a modified version of a previously described technique known as the DPPH assay (Yousaf et al., 2020). The fabricated ZnO-NPs were examined for antioxidant potential against DPPH

at five different doses (20, 30, 40, 50, and 60 $\mu\text{g/mL}$). As a control, ascorbic acid was employed. Briefly, 1 mL of DPPH and 1 mL of sample were mixed together in a test tube, vortexed thoroughly, and left over for half an hour at room temperature. The color change from violet to yellow indicates the antioxidant potential of the sample. 1 mL of DPPH and 1 mL of methanol were combined to make the blank. The absorbance of the reaction mixture was measured at a wavelength of 517 nm. Scavenging activity was calculated using the following equation:

$$\% \text{ scavenging activity} = \frac{(\text{OD control} - \text{OD sample})}{\text{OD control}} \times 100$$

An IC_{50} value was also calculated by plotting % scavenging activity against the concentrations of sample extract. IC_{50} represents the 50 % inhibition at a particular concentration.

2.6. Statistical analysis

The antibacterial and antioxidant data were analyzed for Analysis of Variance of 3 replicates and means were compared for any statistical difference through the least significant difference using the software Statistix 8.1. If the p-value was less than 0.05, the means were substantially different.

3. Results

3.1. Fabrication and characteristics of ZnO-NPs

This study reports the bio-fabrication of ZnO-NPs by using the *Ailanthus altissima* leaf extract. When the plant extract was treated with zinc sulfate solution, a transition in color was observed from yellow to brown with the reaction time, indicating the production of ZnO-NPs. After the successful fabrication of ZnO-NPs, multiple techniques were used to study the physicochemical properties of these NPs. In our results, ZnO-NPs demonstrated an absorbance peak at 327 nm, confirming the formation of ZnO-NPs in the solution (Fig. 1). SEM analysis is further employed to observe the confirmation and morphological characterization of ZnO-NPs. The particles were found to have a predominantly spherical shape (Fig. 2a). Except for ZnO-NPs, no other structure or morphology was found in the synthesized sample. Particles were discovered to be spread in the size range of 1 to 100 nm, with an average size of 13.27 nm (Fig. 2b). The XRD pattern of ZnO-NPs is shown in Fig. 3. The significant peaks at 31.85, 34.45, 34.25, 47.53, 56.52, 62.78, and 67.85 indexed sites to the ZnO hexagonal wurtzite structure's (100), (002), (101), (102), (110), (103), and (112) planes (standard JCPDS card 36-1451). The planes indicate the high

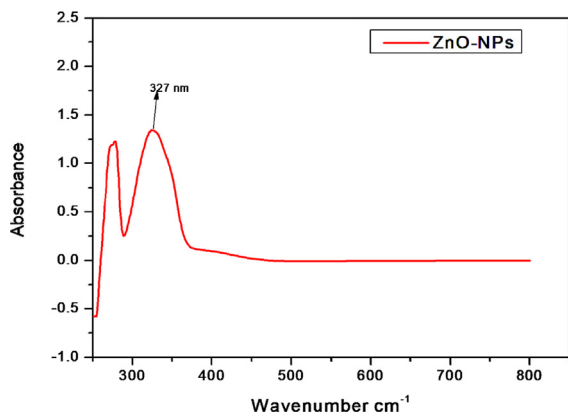


Fig. 1. The UV visible absorption spectrum of ZnO-NPs fabricated from the leaf aqueous extract of *Ailanthus altissima*.

purity and high crystallinity of ZnO-NPs. The interaction between the plant biomolecules and bio-fabricated ZnO-NPs was studied using FTIR. The FT-IR spectra in the range of 4000–500 cm^{-1} was recorded using the KBr pellet technique (Fig. 4). The existence of –OH stretching for phenol is indicated by the band at 3464 cm^{-1} , and the presence of C=O stretch for amides is indicated by the band at 1625 cm^{-1} . The presence of the C–O–H bending mode was confirmed by the peak at 1369 cm^{-1} . The existence of C–C for alkanes is indicated by the peak at 1286 cm^{-1} .

3.2. Antibacterial activity of ZnO-NPs

A dose-dependent bactericidal activity was recorded against gram-positive (*Staphylococcus aureus* and *Streptococcus pyogenes*) and gram-negative (*Escherichia coli* and *Klebsiella pneumoniae*) bacteria. As shown in Fig. 5, concentration-dependent antibacterial zone of inhibition was found against all the tested bacteria. The visual evidence of the zone of inhibition is shown in Fig. 6. An admirable bactericidal activity was observed against all the tested bacteria. However, the highest antibacterial activity (20.33 \pm 0.58 mm) was recorded against *S. aureus* (a gram-positive bacteria) by 20 mg/mL ZnO-NPs. The antibacterial activity was further verified by MIC. ZnO-NPs showed a noteworthy MIC value against all the tested bacteria (Table 1).

3.3. Antioxidant potential

The DPPH radical scavenging experiment was used to determine the antioxidant capacity of the bio-fabricated ZnO-NPs. As shown in Fig. 7, ZnO-NPs showed profound antioxidant activity against DPPH radicals. The percentage of antioxidant activity linearly increases as the concentration of tested samples increases during the reaction. The plant extract has shown much lower antioxidant activity than ZnO-NPs ($P < 0.000$). Fig. 8 shows the IC_{50} value of ZnO-NPs, plant extract, and ascorbic acid (standard). The lower IC_{50} value demonstrates the highest antioxidant activity. In our study, the lower IC_{50} value was found for ascorbic acid (61.75 $\mu\text{g/mL}$), which is a standard antioxidant. However, ZnO-NPs also showed an IC_{50} value (78.23 $\mu\text{g/mL}$) close to ascorbic acid, which means ZnO-NPs have good antioxidant activity.

4. Discussion

Nanotechnology is widely used in different fields and is mostly concerned with the synthesis of NPs of different shapes, sizes, and natures (Remédios et al., 2012). In this study, we fabricated the ZnO-NPs using green synthesis (plant extract). For this, the plant extract was treated with a zinc sulfate solution, and a change in color was noted from yellow to brown, a characteristic of ZnO-NPs in the solution (Otunola et al., 2017). This change is due to the movement of metal ions from a higher to a lower oxidation state (Cuenya, 2010). The bio-fabricated ZnO-NPs were further characterized using different analytical techniques. To begin, the optical properties of ZnO-NPs were explored using UV–visible spectroscopy, which is based on determining a substance's absorbance within a specified wavelength spectrum and is commonly used to validate the presence of a desired component in a sample. As is widely known, metal oxide NPs have significant absorption bands between 200 and 800 nm. In our study, ZnO-NPs exhibited an absorbance peak of 327 nm. SEM confirmed the spherical shape and nano-size (13.27 nm) of ZnO-NPs. Gupta et al. (2018) also confirms the mean size of ZnO-NPs ranging from 1 to 100 nm. The FTIR spectrum confirmed the involvement of biomolecules in the reduction, capping, and stabilizing of ZnO-NPs. There are two main sections in the IR spectrum: the functional group region and the

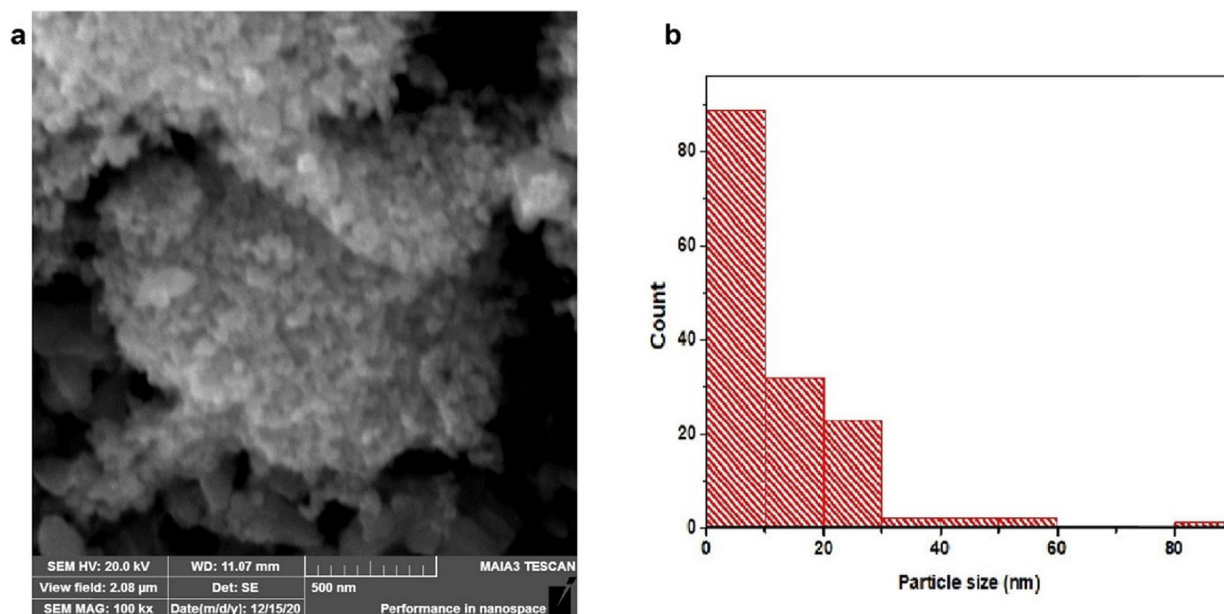


Fig. 2. Morphological characterization of ZnO-NPs, a) SEM micrograph of green synthesized ZnO-NPs, and b) Particle size distribution histogram.

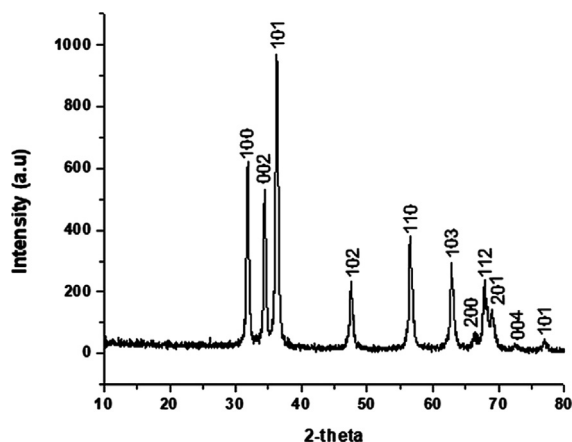


Fig. 3. XRD pattern of green fabricated ZnO-NPs, showing crystalline nature of ZnO-NPs.

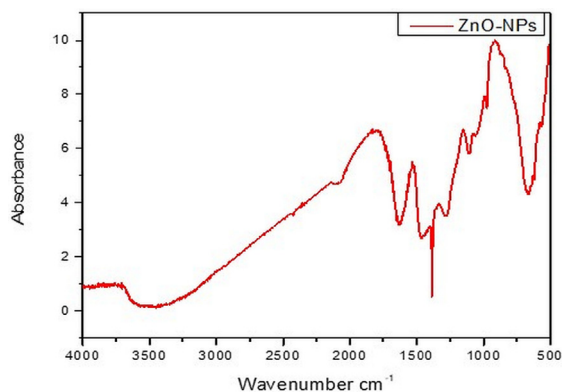


Fig. 4. FTIR spectrum of green fabricated ZnO-NPs.

fingerprint region. The region between 500 and 600 is allotted for a metal–oxygen bond. A relatively small absorption peak at 575 cm^{-1} showed the existence of ZnO-NPs. This region is assigned

to metal–oxygen (Zn–O) vibrations, so it is comparable to another study (Awwad et al., 2020).

Bacterial infections are the most prevalent infections in humans, and they cause a variety of infectious diseases. Nonetheless, these infections can be easily treated with the administration of proper antibiotics. However, widespread and indiscriminate antibiotic use has resulted in an increase in antibiotic resistance among pathogenic bacteria, making antibiotic control problematic (Chandra et al., 2017). The bio-fabricated ZnO-NPs showed excellent bactericidal activity against both gram-positive (*Staphylococcus aureus* and *Streptococcus pyogenes*) and gram-negative (*Escherichia coli* and *Klebsiella pneumonia*) bacteria. However, the higher bactericidal activity was recorded against *S. aureus*, a gram-positive bacterium. These results match with previous studies that biosynthesized ZnO-NPs were highly active antibacterial agents, like ZnO-NPs from leaf extract of *Acalypha fruticosa* L. showed admirable antimicrobial efficacy (Bhavaniramy et al., 2019). However, information about the interaction and penetration of NPs through a bacterial cell wall is still debatable (Schnable et al., 2009). Some possible mechanisms of bacterial growth inhibition by ZnO-NPs are well described. The biomolecules have a greater attraction for the cations that most of the NPs discharge, resulting in an accumulation and bigger uptake of ions, which then cause intracellular destruction (Slavin et al., 2017).

Free radicals are produced during different metabolic processes in the body. However, the overproduction of these free radicals results in oxidative stress that might cause various serious illnesses like cancer, diabetes, cardiovascular, inflammation, and neurodegenerative diseases. Therefore, antioxidant agents are useful in counteracting such problems (Alves et al., 2018). The antioxidant capacity of the test sample was determined by the amount of the conversion of the unstable DPPH solution (blue color) to the stable form (yellow form) (Sujitha et al., 2015). This study discovered that green manufactured ZnO-NPs have notable antioxidant potential. The electron donating capability of the O atom in ZnO-NPs could give their antioxidant capacity (Das et al., 2013). Because of the reducing, capping, and stabilizing agents present on the surface of the NPs, green produced ZnO-NPs have been shown to have excellent antibacterial and antioxidant activities (Ayoughi et al., 2011).

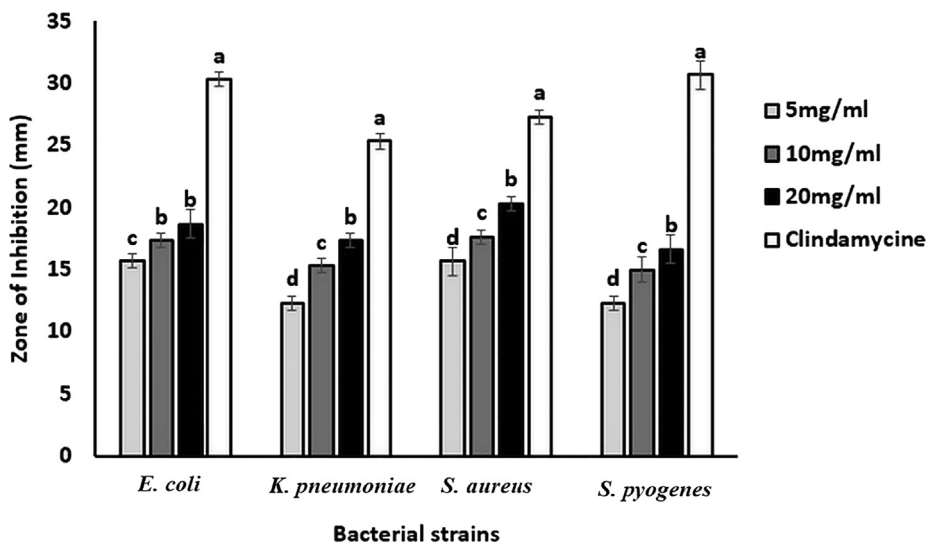


Fig. 5. Antibacterial activity of *Ailanthus altissima* mediated ZnO-NPs and antibiotic (clindamycin) against bacterial pathogens. The values are the averages of 3 replicates, the error bar indicates the standard error of means, and different letters specify a statistically significant difference between the means ($p = 0.05$) using the LSD test.



Fig. 6. Visual evidence of the zone of inhibition of ZnO-NPs against four bacterial strains.

Table 1
MIC values of green synthesized ZnO-NPs.

Concentration of ZnO-NPs	0.3125 mg/mL	0.625 mg/mL	1.25 mg/mL	2.50 mg/mL	5.00 mg/mL	10 mg/mL	20 mg/mL
<i>E. coli</i>	+	-	-	-	-	-	-
<i>K. pneumoniae</i>	+	+	-	-	-	-	-
<i>S. aureus</i>	+	-	-	-	-	-	-
<i>S. pyogenes</i>	+ ₋	+	-	-	-	-	-

Note: (+)-Presence of growth; (-)-Absence of growth.

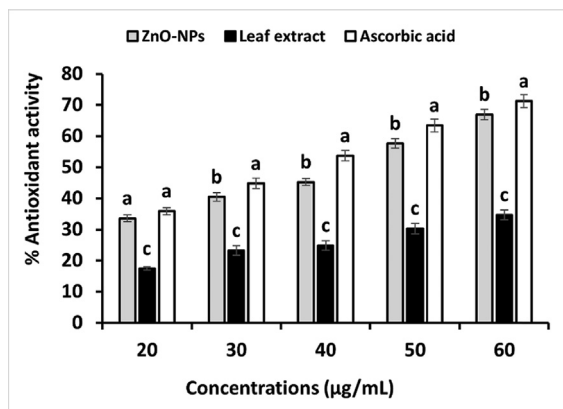


Fig. 7. Antioxidant activity of ZnO-NPs against DPPH. The values are the averages of 3 replicates, the error bar specifies the standard error of means, and different letters specify a statistically significant difference between the means ($p = 0.05$) using the LSD test.

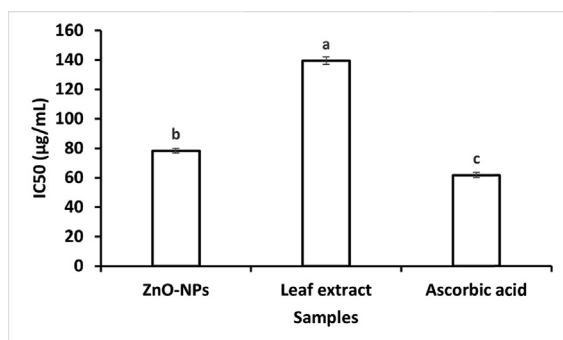


Fig. 8. IC₅₀ value of ZnO-NPs, the values are the averages of 3 replicates, the error bar specifies the standard error of means, and different letters specify a statistically significant difference between the means ($p = 0.05$) using the LSD test.

5. Conclusions

In this study, we used biomolecules from the leaf extract of *Ailanthus altissima* as a capping and stabilizing agent to successfully synthesize spherical ZnO-NPs in a cost-effective, environmentally friendly, and straightforward manner. The synthesized ZnO-NPs were crystalline in nature, spherical in shape, and had an average size of 13.27 nm. FTIR confirms the functional groups involved in the capping and stabilization of ZnO-NPs. The biosynthesized ZnO-NPs inhibited the growth of both gram-positive and gram-negative bacteria. They also showed considerable antioxidant activity. This research demonstrates a cost-efficient and environmentally friendly method for fabricating ZnO-NPs that could be employed as antibacterial and antioxidants. It is necessary to have a thorough understanding of the biochemical processes involved in this plant mediated ZnO NPs synthesis in order to improve the approach's economic viability and sustainability.

Funding

We received no funding from any organization/institution for this study.

Declaration of Competing Interest

The authors declare that they have no known competing financial interests or personal relationships that could have appeared to influence the work reported in this paper.

Acknowledgments

We highly acknowledge the help of the National Institute of Laser Optonics (NILOP) for SEM, EDX, and XRD analysis.

References

- Alves, T.F., Chaud, M.V., Grotto, D., Jozala, A.F., Pandit, R., Rai, M., Dos Santos, C.A., 2018. Association of silver nanoparticles and curcumin solid dispersion: antimicrobial and antioxidant properties. *AAPS PharmSciTech.* 19 (1), 225–231.
- Awwad, A.M., Amer, M.W., Salem, N.M., Abdeen, A.O., 2020. Green synthesis of zinc oxide nanoparticles (ZnO-NPs) using *Ailanthus altissima* fruit extracts and antibacterial activity. *Chem. Int.* 6 (3), 151–159.
- Ayoughi, F., Marzegar, M., Sahari, A.M., Naghdibadi, H., 2011. Chemical compositions of essential oils of *Artemisia dracunculus* L. and endemic *Matricaria chamomilla* L. and an evaluation of their antioxidative effects. *J. Agric. Food Chem.* 1 (679), 79–88.
- Bhavanirama, S., Vishnupriya, S., Al-Aboudy, M.S., Vijayakumar, R., Baskaran, D., 2019. Role of essential oils in food safety: Antimicrobial and antioxidant applications. *Grain Oil Sci. Technol.* 2 (2), 49–55.
- Brooks, M.R., Trifts, V., 2008. Short sea shipping in North America: understanding the requirements of Atlantic Canadian shippers. *Marit. Policy Manag.* 35 (2), 145–158.
- Cao, G., 2004. *Nanostructures & nanomaterials: synthesis, properties & applications.* Imperial College Press.
- Chandra, H., Bishnoi, P., Yadav, A., Patni, B., Mishra, A.P., Nautiyal, A.R., 2017. Antimicrobial resistance and the alternative resources with special emphasis on plant-based antimicrobials—a review. *Plants* 6 (2), 16.
- Cuenya, B.R., 2010. Synthesis and catalytic properties of metal nanoparticles: Size, shape, support, composition, and oxidation state effects. *Thin Solid Films* 518 (12), 3127–3150.
- Das, D., Nath, B.C., Phukon, P., Kalita, A., Dolui, S.K., 2013. Synthesis of ZnO nanoparticles and evaluation of antioxidant and cytotoxic activity. *Coll. Surf. B: Biointerf.* 111 (1), 556–560.
- Fogliatto, S., Milan, M., Vidotto, F., 2020. Control of *Ailanthus altissima* using cut stump and basal bark herbicide applications in an eighteenth-century fortress. *Weed Res.* 60, 425–434.
- Gunalan, S., Sivaraj, R., Rajendran, V., 2012. Green synthesized ZnO nanoparticles against bacterial and fungal pathogens. *Prog. Nat. Sci. Mater. Int.* 22, 693–700.
- Gupta, M., Tomar, R.S., Kaushik, S., Mishra, R.K., Sharma, D., 2018. Effective antimicrobial activity of green ZnO nano particles of *Catharanthus roseus*. *Front. Microbiol.* 9, 2030.
- Iravani, S., 2011. Green synthesis of metal nanoparticles using plants. *Green Chem.* 13 (10), 2638–2650.
- Ishak, N.M., Kamarudin, S., Timmiati, S., 2019. Green synthesis of metal and metal oxide nanoparticles via plant extracts: an overview. *Mater. Res. Exp.* 6, (11) 112004.
- Kim, H.M., Lee, J.S., Sezirahiga, J., Kwon, J., Jeong, M., Lee, D., Choi, J.H., Jang, D.S., 2016. A new canthinone-type alkaloid isolated from *Ailanthus altissima* Swingle. *Molecules* 21, 642.
- Manjunath, K., Ravishankar, T.N., Kumar, D., Priyanka, K., Varghese, T., Raja, N.H., Nagabhushana, H., Sharma, S.C., Dupont, J., Ramakrishnappa, T., Nagaraju, G., 2014. Facile combustion synthesis of ZnO nanoparticles using *Cajanus cajan* (L.) and its multidisciplinary applications. *Mater. Sci. Bull.* 57, 325–334.
- Nilavukkarasi, M., Vijayakumar, S., Prathipkumar, S., 2020. *Capparis zeylanica* mediated bio-synthesized ZnO nanoparticles as antimicrobial, photocatalytic and anti-cancer applications. *Mater. Sci. Energy Technol.* 3, 335–343.

- Otunola, G.A., Afolayan, A.J., Ajayi, E.O., Odeyemi, S.W., 2017. Characterization, antibacterial and antioxidant properties of silver nanoparticles synthesized from aqueous extracts of *Allium sativum*, *Zingiber officinale*, and *Capsicum frutescens*. *Pharmacogn. Mag.* 13 (Suppl 2), S201.
- Remédios, C., Rosário, F., Bastos, V., 2012. Environmental nanoparticles interactions with plants: morphological, physiological, and genotoxic aspects. *J. Bot.* 2012, 751686.
- Schnable, P.S., Ware, D., Fulton, R.S., Stein, J.C., Wei, F., Pasternak, S., Graves, T.A., 2009. The B73 maize genome: complexity, diversity, and dynamics. *Science* 326 (5956), 1112–1115.
- Slavin, Y.N., Asnis, J., Häfeli, U.O., Bach, H., 2017. Metal nanoparticles: understanding the mechanisms behind antibacterial activity. *J. Nanobiotechnol.* 15 (1), 1–20.
- Sujitha, V., Murugan, K., Paulpandi, M., Panneerselvam, C., Suresh, U., Roni, M., Subramaniam, J., 2015. Green-synthesized silver nanoparticles as a novel control tool against dengue virus (DEN-2) and its primary vector *Aedes aegypti*. *Parasitol. Res.* 114 (9), 3315–3325.
- Surmenev, R.A., Orlova, T., Chernozem, R.V., Ivanova, A.A., Bartasyte, A., Mathur, S., Surmeneva, M.A., 2019. Hybrid lead-free polymer-based nanocomposites with improved piezoelectric response for biomedical energy-harvesting applications: A review. *Nano Energ.* 62, 475–506.
- Valdeperas, M., Wiśniewska, M., Ram-On, M., Kesselman, E., Danino, D., Nylander, T., Barauskas, J., 2016. Sponge phases and nanoparticle dispersions in aqueous mixtures of mono-and diglycerides. *Langmuir* 32 (34), 8650–8659.
- Yang, X.L., Yuan, Y.L., Zhang, D.M., Li, F., Ye, W.C., 2014. Shinjulactone O, a new quassinoid from the root bark of *Ailanthus altissima*. *Nat. Prod. Res.* 28, 1432–1437.
- Yousaf, H., Mehmood, A., Ahmad, K.S., Raffi, M., 2020. Green synthesis of silver nanoparticles and their applications as an alternative antibacterial and antioxidant agents. *Mat. Sci. Eng.: C* 112.
- Zhang, L., Jiang, Y., Ding, Y., Povey, M., York, D., 2007a. Investigation into the antibacterial behaviour of suspensions of ZnO nanoparticles (ZnO nanofluids). *J. Nanopart. Res.* 9 (3), 479–489.
- Zhang, L.P., Wang, J.Y., Wang, W., Cui, Y.X., Cheng, D.L., 2007b. Two new alkaloidal glycosides from the root bark of *Ailanthus altissima*. *J. Asian Nat. Prod. Res.* 9, 253–259.